

# Laser-driven ion accelerators: Spectral control, monoenergetic ions and new acceleration mechanisms

K. FLIPPO,<sup>1</sup> B.M. HEGELICH,<sup>1</sup> B.J. ALBRIGHT,<sup>1</sup> L. YIN,<sup>1</sup> D.C. GAUTIER,<sup>1</sup> S. LETZRING,<sup>1</sup>  
M. SCHOLLMEIER,<sup>2</sup> J. SCHREIBER,<sup>3</sup> R. SCHULZE,<sup>1</sup> AND J.C. FERNÁNDEZ<sup>1</sup>

<sup>1</sup>Los Alamos National Laboratory, Los Alamos, New Mexico

<sup>2</sup>Darmstadt Technische Universität, Darmstadt, Germany

<sup>3</sup>LMU Muenchen, Muenchen, Germany

(RECEIVED 12 August 2006; ACCEPTED 25 September 2006)

## Abstract

Los Alamos National Laboratory short pulse experiments have shown using various target cleaning techniques such that heavy ion beams of different charge states can be produced. Furthermore, by controlling the thickness of light ions on the rear of the target, monoenergetic ion pulses can be generated. The spectral shape of the accelerated particles can be controlled to yield a range of distributions, from Maxwellian to ones possessing a monoenergetic peak at high energy. The key lies in understanding and utilizing target surface chemistry. Careful monitoring and control of the surface properties and induction of reactions at different temperatures allows well defined source layers to be formed, which in turn lead to the desired energy spectra in the acceleration process. Theoretical considerations provide understanding of the process of monoenergetic ion production. In addition, numerical modeling has identified a new acceleration mechanism, the laser break-out afterburner that could potentially boost particle energies by up to two orders of magnitude for the same laser parameters. This mechanism may enable application of laser-accelerated ion beams to venues such as compact accelerators, tumor therapy, and ion fast ignition.

**Keywords:** Break-out afterburner; Enhanced TNSA; Fast ignition fusion; Femtosecond lasers; Laser ion acceleration; Laser-plasma interactions; Monoenergetic ion beam; Short-pulse lasers; Target normal sheath acceleration

## 1. INTRODUCTION

The study of short-pulse laser accelerated ions (Snavely *et al.*, 2000; Clark *et al.*, 2000; Maksimchuk *et al.*, 2000; Krushelnick *et al.*, 2000) has seen rapid progress in recent years as seen with the acceleration of heavier ion species by cleaning the hydrogenic compounds off the target by ohmic heating (Hegelich *et al.*, 2002), ion sputter etch cleaning (Allen *et al.*, 2004), and laser heating and laser ablation (Fernández *et al.*, 2005; Flippo *et al.*, 2006). Also progress has been made in the characterization of the accelerating sheath (Brambrink *et al.*, 2006), which leads to superior beam quality seen from short-pulse laser sources as compared to conventional accelerators (Roth *et al.*, 2005; Ruhl *et al.*, 2006). But the most potentially useful advances are in the realm of energy spectral control, like the recent observation of monoenergetic carbon beams (Hegelich *et al.*,

2006), the quasi-monoenergetic population enhancement in the proton spectra (Schwoerer *et al.*, 2006), and a new enhanced acceleration regime, the break-out afterburner (BOA) was recently reported by Yin *et al.* (2006).

Up to now, the majority of high energy ions have been accelerated by the target normal sheath acceleration (TNSA) mechanism (Hatchett *et al.*, 2000; Wilks *et al.*, 2001), which has led to maximum energies of 58 MeV for protons (Snavely *et al.*, 2000), 100 MeV for  $F^{+7}$  (Hegelich *et al.*, 2002), 200 MeV for  $Pd^{+22}$  (Fernández *et al.*, 2005; Hegelich *et al.*, 2005), and  $\sim 40$  MeV for the quasi-monoenergetic beam of  $C^{+5}$  (Hegelich *et al.*, 2006). The Plasma Physics group at Los Alamos National Laboratory is embarking on a program to produce high quality tunable ion beams for research into fast ignition and ion stopping power in plasmas. To this end, experiments on heavy ion beams, monoenergetic carbon beams, other heavy ion beams, and beam spectral and spatial control are currently being carried out using various methods to control beam parameters. In addition, computer simulations have demonstrated production of GeV ions from

Address correspondence and reprint requests to: Kirk Flippo, Los Alamos National Laboratory, MS E526, Los Alamos, New Mexico 87545. kflippo@lanl.gov

BOA acceleration. Experimental realization of the BOA, with optimization of target thickness and laser parameters, is being considered as well.

In this paper, we discuss techniques for surface preparation and cleaning as well as spectral control, and optimization of beam energy. In Section 2, we present results showing how laser ablation of contaminants on surfaces can be used, both in isolation and in concert with other methods (for example, ohmic heating), to control target surface properties. In Section 3, we describe the application of these methods to the generation of monoenergetic ion spectra via the production of a carbon monolayer onto a palladium substrate. We also show particle-in-cell simulation results of the BOA, involving the use of a high-contrast ratio, high intensity laser, and a very thin target foil.

## 2. SURFACE PREPARATION AND CLEANING TO ENABLE ION SPECIES AND SPECTRAL CONTROL

It has been known since the 1970s that the target surface conditions are important to the species of ion accelerated (Joshi *et al.*, 1979). Typical non-treated targets have a contamination layer on the surface, which is the source of the protons seen in the first short-pulse ion acceleration experiments. The contamination layer is typically on the order of a few  $10^{16}$  atoms/cm<sup>2</sup> of CHO, corresponding to many monolayers of surface contamination (Fernández *et al.*, 2005). These hydrogenic (H<sub>2</sub>O and CH) compounds can be easily removed from targets that can withstand high temperatures (> 900°C), however, this limits the choice of target material. Not only does one have to choose targets that can

withstand the heat, but also targets that do not form other native layer compounds such as oxides, carbides, or nitrides. These layers typically have binding energies well above 1 eV and can withstand temperatures well in excess of the bulk target material, proving very difficult to remove. Ideally one would like to have an arbitrary choice of energy spectrum and material from which to produce an ion beam. This calls for a solution that can remove the contamination layer along with any native oxide, carbide, or nitride layer, to leave only the substrate ions to be accelerated.

Laser ablation is an obvious candidate to solve these problems. The Trident facility is capable of firing three beams simultaneously. C-beam is configured as the short-pulse beamline, 20 J in 600 fs; A- and B-beams are long-pulse beams and can be configured from 1  $\mu$ s to 100 ps, and up to 200 J depending on the pulse duration. One long-pulse beam at 150 ps was used to ablate the target 20 ms before the short-pulse arrived. This temporal spacing was chosen to minimize recontamination of the surface between the pulses. Simulations together with previous ablation experiments (Flippo *et al.*, 2006; Fernández *et al.*, 2005) led to the determination that an intensity of between  $5 \times 10^{10}$  and  $1 \times 10^{11}$  W/cm<sup>2</sup> would yield the best results. Vanadium was chosen as a target material because the short-pulse should be able to ionize it to a Li-like state for maximum acceleration efficiency and vanadium forms strong oxides, which will test the ablation principle.

Normally when an unablated, unheated vanadium target is shot with short-pulse driver beam at  $2 \times 10^{19}$  W/cm<sup>2</sup>, a very strong proton signal is seen. Typical results from a cold vanadium target proton beam intercepting a stack of RCF is shown in Figure 1. Each film layer corresponds to a different

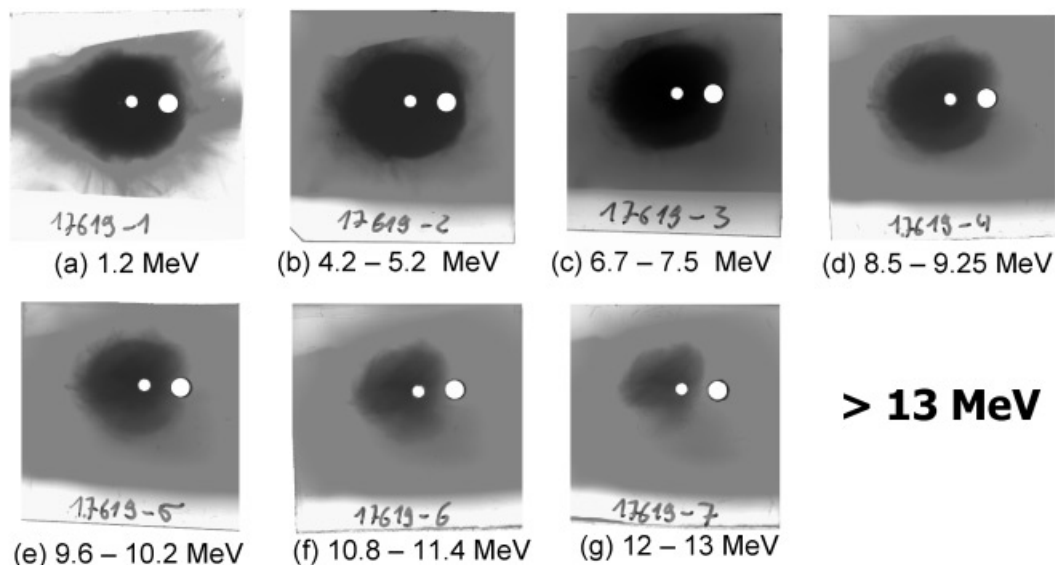


**Fig. 1.** A detector stack of radiochromic film (RCF) used to diagnose the proton beam. Each layer corresponds to a different energy range of protons dependent upon the Bragg peak. The darkest portion of each film is the proton beam. The first film is GAF-HD810, a less sensitive film; subsequent films are GAF-MD55. Two holes were cut out of the film stack to allow ions to enter the TP detectors.

energy slice of the proton beam, determined by the Bragg peak, the point of greatest stopping power and hence energy deposition for that proton energy in the RCF stacks. The RCF stack shows a proton beam whose energy is greater than 13 MeV. The first film in the stack was a thinner film (Gafchromic HD-810), which is not as sensitive to the protons, and thus has a slightly lighter and smaller profile. The next six films were composed of a more sensitive type of film (Gafchromic MD-55). The two holes are provided to allow the ions to enter two Thomson parabolas (TP) (Thomson, 1911), which are mass spectrometers with parallel magnetic and electric fields, separating the ions into parabolic traces corresponding to different charge to mass ratios. The ions are recorded on a nuclear track detector CR-39 placed in the TP.

When a proton beam is produced from an untreated target, it limits the type and number of species that can be accelerated since the TNSA mechanism can simply be thought of as an electrostatic potential. For example, only the lowest charge states of vanadium are present (usually not above  $V^{+4}$ ), however heating a target to above  $900^{\circ}\text{C}$  leads to a reduction in the proton signal that allows for higher charge states of vanadium and more energetic energy spectrum. Charge states up to  $V^{+7}$  have been observed from purely heated targets. However, carbon, and oxygen are still present in quantity and acquire energy that could have been transferred to the vanadium, limiting the efficiency. When the target is heated sufficiently by a CW 527 nm laser, the proton beam can be nearly eliminated and does not have sufficient energy to penetrate the aluminum cover on the first film, shown in Figure 2a, and has been reduced to less than 0.2 MeV, which is the detection threshold of the CR-39 in the TP. The signal on the RCF in Figure 2a is from energetic carbon and/or oxygen ions, also seen on the TP, leading to the conclusion that just because protons are not observed on the RCF, this doesn't mean the target was clear of carbon and oxygen.

The ablation beam should rid the surface of all contaminants without destroying the bulk target, allowing the bulk material to be ionized to high Z and accelerated. The TP was used to determine the ion energies and species originating from the targets. When the ablation beam was used, the target could not be heated as rigorously because it was then not mechanical strong enough to survive the ablation beam. Thus, when the ablation beam and medium heating (below  $\sim 800^{\circ}\text{C}$ ) were applied, protons were still present, however the number of protons and their energy were reduced significantly, but not eliminated, as shown in Figure 3, but still orders of magnitude in number above the vanadium. The protons most likely originate from the bulk of the material as the target was only heated for less than 10 min, not allowing for complete desorption, or were possibly pushed into the target by the ablation process. The proton energy dropped from above 13 MeV to less than 1 MeV, and the total laser energy transferred to the protons is down from about 1% to less than 0.03%. The reduced presence of the protons had a dramatic result, the maximum ionization state of vanadium

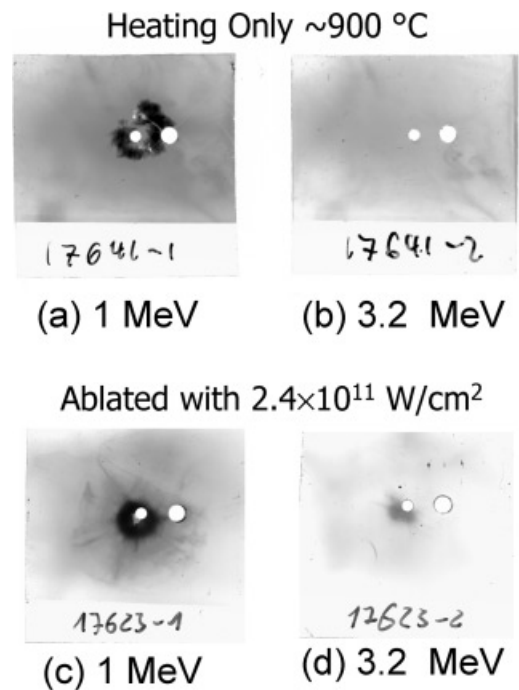


**Fig. 2.** RCF (GAF HD-810) stacks from two shots, (a) and (b) are from a Vanadium target heated to  $900^{\circ}\text{C}$ , but not ablated; (c) and (d) is a beam from a target that was ablated with  $2.4 \times 10^{11} \text{ W/cm}^2$  and heated to  $\sim 800^{\circ}\text{C}$ . Energies given are for protons.

ion species and their maximum cutoff energies were increased from  $V^{+7}$  to  $V^{+17}$  and from 18 MeV to 35 MeV, respectively, with 0.13% of the laser energy converted into the  $V^{+17}$  charge state alone. Oxygen and carbon are again present in this heated plus ablated shot, but reduced in number and increased in energy and charge state. Due to the resolution

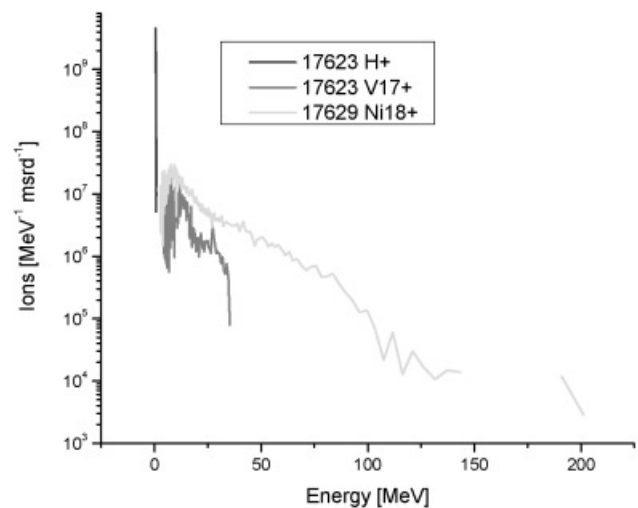


**Fig. 3.** Ion number [ /MeV/msrd ] vs. energy for a heated plus ablated shot (17623) showing the short, low energy proton spectra (blue) and the high energy  $V^{+17}$  spectrum (red), and an energy spectrum from  $Ni^{+18}$  on a simple heated shot (17629, green) of a noble metal.

of the detector, it is not possible to resolve the charge to mass difference for all the high energy vanadium, oxygen, and carbon species. Consequently, once again this signal in Figure 2c and 2d are likely from carbon and oxygen impurities not removed from the heated and ablated target, however, they are now energetic enough to penetrate the second layer of RCF, which is consistent with the TP signal corresponding to carbon at 4.5 MeV/nucleon.

Figure 3 also shows that a target such as nickel, which is termed a noble metal for its propensity to not form compounds readily in air and to form only a weak oxide, is when heated to 1000°C, able to drive off the protons as well as most of the carbon, and also doesn't have a large native population of oxygen, thus much more of the laser energy can be transferred to the nickel ions, 0.8% into  $\text{Ni}^{+18}$  alone. The efficiency of the noble metal indicates that the ablation technique still needs to be optimized by possibly longer target heating and perhaps higher energy ablation photons, that is, UV.

### 3. MONOENERGETIC IONS AND THE FUTURE

The same heating technique, described above with nickel, when applied to a strong catalytic metal such as palladium or platinum, can lead to the creation of a very thin layer of graphitic carbon when properly controlled. This layer is the source for the production of multi MeV/nucleon monoenergetic carbon ions (Hegelich *et al.*, 2006) when such a target is irradiated with a high intensity laser beam. Theoretical understanding of monoenergetic beam production indicates that the dynamics are largely 1D during the early phases of the expansion, with the sheath electric fields providing the sources of ionization (via field ionization) and acceleration.

The monoenergetic beam energy and the energy of the substrate are controlled by the hot electron temperature, the aerial charge density of the light ion layer, and the compositions of the beam and substrate. The thickness and transverse size of the source layer control the spread of the monoenergetic beam and therefore the beam quality (Albright *et al.*, 2006a, 2006b).

We are currently working to extend monoenergetic ion production to a range of ion species and much higher energy and conversion efficiency (laser energy to ion beam energy) with a new scheme, termed the BOA (Yin *et al.*, 2006). One-dimensional particle-in-cell simulations using the Los Alamos National Laboratory VPIC code show that with the use of careful target preparation and laser conditioning, carbon ions can be accelerated to energies exceeding 1 GeV when the target thickness is comparable to the electron skin depth. In the study, a very thin ( $\sim 30$  nm) target is irradiated by a very high contrast, high-intensity ( $I \sim 10^{21}$  W/cm<sup>2</sup>) laser pulse. Initially, the laser accelerates electrons from the solid target to generate a sheath on the rear target surface, as in the TNSA mechanism. However, with very thin targets, the population of cold electrons is rapidly depleted and return current to the laser deposition layer is provided by refluxing hot electrons, which further heat. This “enhanced TNSA” process a few 10 s of fs from the start of TNSA acceleration, and the laser efficiently heats the entire column of hot electrons in the target layer. The hot electrons' temperature rapidly increases as the layer expands, and the layer ultimately becomes transparent to the laser. When the laser penetrates the target and directly interacts with the electrons at the rear, a large electrostatic field at the rear is formed with a peak that co-moves with the ions, causing the ions to receive a large impulse and accelerate as a quasi-

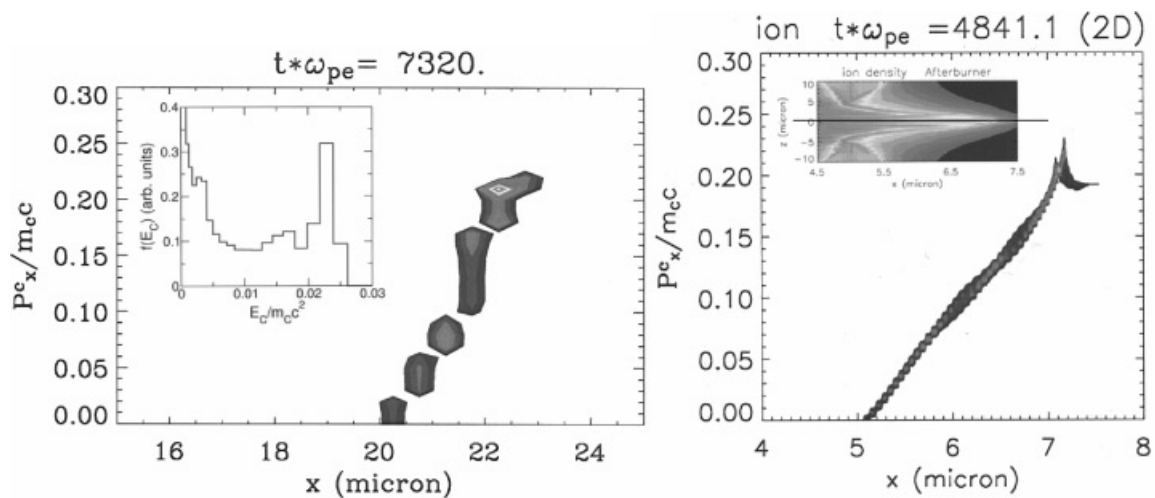


**Fig. 4.** (left) 1D PIC simulation showing momentum vs. position for carbon ions accelerated by the BOA mechanism. A monoenergetic feature in the spectrum is apparent from the inset (right) 2D PIC simulation of the BOA preserves the monoenergetic feature and exhibits comparable beam energy. The inset shows the ion density distribution in 2D where the initial target (30 nm thick) is centered at  $x = 5 \mu\text{m}$  initially and the black line is the line-out used for the main plot.

monoenergetic bunch, seen in Figure 4 (left) as a bright red and yellow spot in the ion population, and again in the inset as the peak in number at the high energy end of the spectrum. This is the “afterburner” phase of the accelerator. Later evolution of the afterburner widens the energy spectrum and promotes the fastest ions to very high ( $> \text{GeV}$ ) energies. The generic features of the BOA mechanism have been observed in two-dimensional simulations, which preserve the monoenergetic feature (Fig. 4, right). (The monoenergetic beam component is the small dense feature in phase space near  $7 \mu\text{m}$  and  $0.2 \text{ p/mc}$ ). We note that if target cleaning is required for BOA operation, delicacy of these targets may pose additional challenges for its realization.

#### 4. SUMMARY

We have shown that techniques for surface preparation and cleaning, using laser ablation of contaminants on the rear surface in concert with joule laser heating, can reduce the proton number and energy while increasing the vanadium charge states and energy, and also showed that removing the hydrogen alone from targets with oxide layers is not sufficient to significantly improve the transfer of laser energy to heavy ions. The creation of a carbon monolayer on a palladium target through catalytic heating was shown to generate monoenergetic ions, and modeling has shown that by controlling this layer one can control the ion spectral shape. Particle-in-cell simulation results of the BOA, involving the use of a high-contrast ratio, high intensity laser, and a very thin target foil have shown the potential to accelerate ions to GeV energies. All these techniques being developed are the beginnings of high quality laser ion accelerators with precision ion specie and spectral control.

#### REFERENCES

ALBRIGHT, B.J., YIN, L., KWAN, T.J.T., BOWERS, K.J., HEGELICH, B.M. & FERNÁNDEZ, J.C. (2006a). Theory and modelling of ion acceleration from the interaction of ultra-intense lasers with solid density targets. *J. Phys. IV France* **133**, 467–471.

ALBRIGHT, B.J., YIN, L., HEGELICH, B.M., BOWERS, KEVIN, J., KWAN, T.J.T. & FERNÁNDEZ, J.C. (2006b). Theory of laser acceleration of light ion beams from interaction of ultrahigh intensity lasers with layered targets. *Phys. Rev. Lett.* **97**, 115002.

ALLEN, M., PATEL, P.K., MACKINNON, A., PRICE, D., WILKS, S. & MORSE, E. (2004). Direct experimental evidence of back surface ion acceleration from laser-irradiated gold foils. *Phys. Rev. Lett.* **93**, 265004.

BRAMBRINK, E., ROTH, M., BLAZEVIC, A. & SCHLEGEL, T. (2006). Modeling of the electrostatic sheath shape on the rear target surface in short-pulse laser-driven proton acceleration. *Laser Part. Beams* **24**, 163–168.

CLARK, E.L., KRUSHELNICK, K.R., DAVIES, J., ZEPF, M., TATARAKIS, M., BEG, F.N., MACHACEK, A., NORREYS, P.A., SANTALA, M.I.K., WATTS, I. & DANGOR, A.E. (2000). Measurements of energetic proton transport through magnetized plasma from intense laser interactions with solids. *Phys. Rev. Lett.* **84**, 670.

FERNÁNDEZ, J.C., HEGELICH, B.M., COBBLE, J.A., FLIPPO, K.A., LETZRING, S.A., JOHNSON, R.P., GAUTIER, D.C., SHIMADA, T., KYRALA, G.A., WANG, Y., WETTLAND, C.J. & SCHREIBER, J. (2005). Laser-ablation treatment of short-pulse laser targets: Toward an experimental program on energetic-ion interactions with dense plasmas. *Laser Part. Beams* **23**, 267.

FLIPPO, K.A., HEGELICH, B.M., SCHMITT, M.J., MESEROLE, C.A., COBBLE, J.A., FISHER, G.L., GAUTIER, D.C., JOHNSON, R., LETZRING, S., SCHREIBER, J., SCHOLLMEIER, M. & FERNÁNDEZ, J.C. (2006). Ultrashort-Laser-Produced Heavy Ion Generation via Target Laser-Ablation Cleaning. *J. Phys. IV France* **133**, 1117.

HATCHETT, S.P., BROWN, C.G., COWAN, T.E., HENRY, E.A., JOHNSON, J.S., KEY, M.H., KOCH, J.A., LANGDON, A.B., LASINSKI, B.F., LEE, R.W., MACKINNON, A.J., PENNINGTON, D.M., PERRY, M.D., PHILLIPS, T.W., ROTH, M., SANGSTER, T.C., SINGH, M.S., SNAVELY, R.A., STOYER, M.A., WILKS, S.C. & YASUIKE, K. (2000). Electron, photon, and ion beams from the relativistic interaction of Petawatt laser pulses with solid targets. *Phys. Plasma* **7**, 2076.

HEGELICH, B.M., KARSCH, S., PRETZLER, G., HABS, D., WITTE, K., GUENTHER, W., ALLEN, M., BLAZEVIC, A., FUCHS, J., GAUTHIER, J.C., GEISSEL, M., AUDEBERT, P., COWAN, T. & ROTH, M. (2002). MeV ion jets from short-pulse-laser interaction with thin foils. *Phys. Rev. Lett.* **89**, 085002.

HEGELICH, B.M., ALBRIGHT, B., AUDEBERT, P., BLAZEVIC, A., BRAMBRINK, E., COBBLE, J., COWAN, T., FUCHS, J., GAUTHIER, J.C., GAUTIER, C., GEISSEL, M., HABS, D., JOHNSON, R., KARSCH, S., KEMP, A., LETZRING, S., ROTH, M., SCHRAMM, U., SCHREIBER, J., WITTE, K.J. & FERNÁNDEZ, J.C. (2005). Spectral properties of laser-accelerated mid-Z MeV/u ion beams. *Phys. Plasmas* **12**, 056314.

HEGELICH, B.M., ALBRIGHT, B., COBBLE, J., FLIPPO, K., JOHNSON, R., LETZRING, S., PAFFETT, M., RUHL, H., SCHREIBER, J., SCHULZE, R. & FERNANDEZ, J.C. (2006). Mono-energetic multi-MeV/nucleon ion beams accelerated by ultrahigh intensity lasers. *Nature* **439**, 441–444.

JOSHI, C., RICHARDSON, M.C. & ENRIGHT, G.D. (1979). Quantitative measurements of fast ions from  $\text{CO}_2$  laser-produced plasmas. *Appl. Phys. Lett.* **34**, 625.

KRUSHELNICK, K., CLARK, E.L., ZEPF, M., DAVIES, J.R., BEG, F.N., MACHACEK, A., SANTALA, M.I.K., TATARAKIS, M., WATTS, I., NORREYS, P.A. & DANGOR, A.E. (2000). Energetic proton production from relativistic laser interaction with high density plasmas. *Phys. Plasma* **7**, 2055.

MAKSIMCHUK, A., GU, S., FLIPPO, K., UMSTADTER, D. & BYCHENKOV, V.YU. (2000). Forward ion acceleration in thin films driven by a high-intensity laser. *Phys. Rev. Lett.* **84**, 4108.

ROTH, M., BRAMBRINK, E., AUDEBERT, P., BLAZEVIC, A., CLARKE, R., COBBLE, J., COWAN, T.E., FERNANDEZ, J., FUCHS, J., GEISSEL, M., HABS, D., HEGELICH, M., KARSCH, S., LEDINGHAM, K., NEELY, D., RUHL, H., SCHLEGEL, T. & SCHREIBER, J. (2005). Laser accelerated ions and electron transport in ultra-intense laser matter interaction. *Laser Part. Beams* **23**, 95–100.

RUHL, H., COWAN, T. & PEGORARO, F. (2006). The generation of images of surface structures by laser-accelerated protons. *Laser Part. Beams* **24**, 181–184.

SNAVELY, R.A., KEY, M.H., HATCHETT, S.P., COWAN, T.E., ROTH, M., PHILLIPS, T.W., STOYER, M.A., HENRY, E.A., SANGSTER, T.C., SINGH, M.S., WILKS, S.C., MACKINNON, A., OFFENBERGER, A., PENNINGTON, D.M., YASUIKE, K., LANGDON,

- A.B., LASINSKI, B.F., JOHNSON, J., PERRY, M.D. & CAMPBELL, E.M. (2000). Intense high-energy proton beams from petawatt laser irradiation of solids. *Phys. Rev. Lett.* **85**, 2945.
- SCHWOERER, H., PFOTENHAUER, S., JÄCKEL, O., AMTHOR, K.-U., LIESFELD, B., ZIEGLER, W., SAUERBREY, R., LEDINGHAM, K.W.D. & ESIRKEPOV, T. (2006). Laser–plasma acceleration of quasi-monoenergetic protons from microstructured targets. *Nature* **439**, 445.
- THOMSON, J.J. (1911). Rays of Positive Electricity. *Phil. Mag.* **21**, 255.
- WILKS, S.C., LANGDON, A.B., COWAN, T.E., ROTH, M., SINGH, M., HATCHETT, S., KEY, M.H., PENNINGTON, D., MACKINNON, A. & SNAVELY, R.A. (2001). Energetic proton generation in ultra-intense laser–solid interactions. *Phys. Plasma* **8**, 542.
- YIN, L., ALBRIGHT, B.J., HEGELICH, B.M. & FERNÁNDEZ, J.C. (2006). GeV laser ion acceleration from ultrathin targets: The laser break-out afterburner. *Laser Part. Beams* **24**, 291–298.